
SINGLE PASS COLLIDER MEMO CN-339

AUTHOR: W. Weng and M. Sands

DATE: Nov. 14, 1986

TITLE: **DISPERSIVE EFFECTS OF ORBIT ERRORS IN THE
SLC ARCS***

TABLE OF CONTENTS

- I. The Unperturbed off-Energy Functions
- II. The Perturbed off-Energy Functions with Coupling
- III. Excitation of Eta by Trajectory Errors
- IV. Anomalous Eta after Steering Corrections
- V. Numerical Estimates
- VI. Discussions

** This material is based upon work supported by the U.S. Department of Energy,
Office of Science, under Contract No. DE-AC02-76SF00515.*

INTRODUCTION

The behavior of the off-energy functions of the arcs determines the extent of the emittance growth in the arc and the amount of residual dispersion at the IP. For a perfect machine, with no field and alignment errors, the emittance growth in the arc is about 30% in the horizontal plane and 6% in the vertical plane. A nine-parameter linear optical correction system is provided in the beginning of Final Focus to correct optical errors introduced by nominal misalignment and field errors in the arcs. This report is an analytical attempt to estimate the perturbations of eta-functions after orbit correction.

There are many factors affecting the off-energy functions in the SLC arcs. In this report we will concentrate on the effects caused by the orbit errors created by misalignments. Because the dipole, quadrupole and sextupole components are all present in all arc magnets, any orbit error will introduce both bending and gradient errors which modify the dispersion functions. It will be shown that the 'non-dispersive' property of a 'magnet mover' is not true whenever the vertical off-energy function is non-zero.

Although the lattice structures of the two arcs are not exactly identical, the properties in their overall behavior are very similar. In the following discussion the north arc will be used as an example for numerical estimation. The same analysis can be applied to the south arc, and the result should be similar to that of the north. In this report the term off-energy functions, dispersion functions and eta functions will be used interchangeably.

I. The Unperturbed Off-Energy Functions.

The north arc of the SLC consists of 22 regular achromats and one special section, the north reverse bend insertion. Each regular achromat consists of 10 basic FODO cells, and each cell is composed of two combined function magnets, each having superimposed dipole, quadrupole and sextupole fields. To follow

the terrain of the SLC site, selective achromats are rolled to guide the particle in the vertical plane in addition to the more or less constant horizontal bending.

In every achromat, the horizontal off-energy function is a periodic solution of the differential equation^{(1),(2)},

$$\eta_x'' + K_x(s)\eta_x = G_x(s) \quad (1)$$

where $G_x(s)$ is the curvature function, and $K_x(s)$ is the focusing function defined as,

$$G_x(s) = \frac{1}{\rho}, \quad K_x(s) = \frac{1}{B\rho} \frac{dB_y}{dx} + \frac{1}{\rho^2} \quad (2)$$

The solution as shown in Fig. 1 is a periodic function with maximum value of 47.42 mm in the middle of a focus magnet and a minimum value of 22.73 mm in the middle of a defocus magnet.

For those achromats which have no roll, because there is no bending in the vertical plane, the vertical off-energy function is zero everywhere. If the achromat as a whole is rolled with respect to the beam axis by an angle θ , there will be vertical dispersion created in that achromat due to the mismatch created at the boundary from one achromat to another. The transition from one achromat to another is illustrated in Fig. 2.

Before entering the first achromat of the north arc, the beam coordinate system is the same as that of the Linac designated as (X, Y) . The first achromat of the north arc is rolled -10° with respect to the longitudinal direction Z , and the new beam coordinate system is designated as (X_1, Y_1) . There are two ways of finding the vertical dispersion function in achromat one. The first is to continue using (X, Y) as a coordinate system, expressing magnetic fields in (X, Y) and solving the coupled equation of motion in the (X, Y) frame. The second approach is to recognize the fact that if we use the (X_1, Y_1) frame as the new coordinate system, there is no vertical bending and, therefore, again no new

dispersion to be generated within (X_1, Y_1) . However, the initial conditions of the dispersion function now appear both in horizontal and vertical planes. They will propagate along the first achromat as free betatron oscillation. It is much easier to solve two independent betatron oscillations than solving a coupled equation of motion. Here we adopt the second approach.

Again, using the north arc as an example, the horizontal dispersion function at the end of the defocus magnet, which is upstream of the entrance of the first achromat, is

$$\begin{pmatrix} \eta_x \\ \eta'_x \end{pmatrix}_D = \begin{pmatrix} 34.58 \text{ mm} \\ 18.31 \text{ mrad} \end{pmatrix}, \quad \begin{pmatrix} \eta_y \\ \eta'_y \end{pmatrix}_D = \begin{pmatrix} 0 \\ 0 \end{pmatrix} \quad (3)$$

In the (X_1, Y_1) frame, the initial conditions of the dispersion functions at the entrance of the first F magnets can be found from the upstream magnet by a rotation of angle θ ,

$$\begin{pmatrix} \eta_{x1} \\ \eta_{y1} \end{pmatrix}_F = \begin{pmatrix} \cos\theta & \sin\theta \\ -\sin\theta & \cos\theta \end{pmatrix} \begin{pmatrix} \eta_x \\ \eta_y \end{pmatrix}_D \quad (4)$$

where θ is the roll angle. The same equations apply to (η'_{x1}, η'_{y1}) pair. Putting the roll of $\theta_1 = -10^\circ$ in Eqs. (3) and (4), we obtain

$$\begin{pmatrix} \eta_{x1} \\ \eta'_{x1} \end{pmatrix}_F = \begin{pmatrix} 34.1 \text{ mm} \\ 18.0 \text{ mrad} \end{pmatrix}, \quad \begin{pmatrix} \eta_{y1} \\ \eta'_{y1} \end{pmatrix}_F = \begin{pmatrix} 6.0 \text{ mm} \\ 3.18 \text{ mrad} \end{pmatrix} \quad (5)$$

In the (X_1, Y_1) frame, the horizontal dispersion function is still very well matched and will be more or less the same as there is no roll; the vertical dispersion function will be the free betatron oscillation generated by initial conditions given in Eq. (5). The amplitude of the oscillation can be found through the following expression ⁽¹⁾.

$$a^2 = \frac{\eta_{y1}^2}{\beta_y} + \beta_y \left(\eta_{y1}' - \frac{\beta_y'}{2\beta_y} \eta_{y1} \right)^2 \quad (6)$$

Therefore the maximum amplitude of the vertical off-energy function is approximately

$$\eta_{y1,max} \approx \sqrt{\beta_{ymax}} a \approx 42.0mm$$

Consequently, this vertical dispersion function will oscillate between -42 mm and 42 mm three times within the first achromat, as shown in the η_y plot of Fig. 1a.

At the end of first achromat, a local right-handed beam following coordinate system can be established, which is the same as used in TRANSPORT⁽³⁾ for calculating transfer matrix and will be called (\bar{X}_1, \bar{Y}_1) , see Fig. 2. For definition and explanation for the coordinate system, please read Type code 20 in the TRANSPORT manual. For a perfect machine, the phase advance within one achromat, from (X, Y) frame to (\bar{X}_1, \bar{Y}_1) frame is 6π which means that the transfer matrix for the dispersion function is simply a unit matrix. Therefore, at the end of first achromat, in the (\bar{X}_1, \bar{Y}_1) frame, the dispersion function will reproduce its condition at the entrance to the first achromat, *i.e.*, a vector in horizontal plane.

If the second achromat has no roll with respect to the (\bar{X}_1, \bar{Y}_1) frame, there will be no vertical dispersion in the second achromat following the first one. On the other hand, if the second achromat has relative roll with respect to (\bar{X}_1, \bar{Y}_1) frame, then there will be a mismatch resulting in residual off-energy function in the second achromat as well.

To summarize, the unperturbed horizontal off-energy function in the north arc is a periodic function with a FODO cell as a fundamental period. The unperturbed vertical dispersion function is a free betatron oscillation created by the roll in the beginning of each achromat. The amplitude is about 42 mm for 10° of roll. The design rolls and the maximum amplitudes of vertical dispersions of the north arc are tabulated in Table I. Both horizontal and vertical off-energy functions of the arc are plotted in Fig. 1 which are taken from the SLC Design

Handbook.⁽⁴⁾

From Table I, It is worth pointing out that in the north arc, there are nine achromats with zero unperturbed vertical dispersions, six with maximum vertical dispersion around 20 ~ 30 mm and eight achromats with maximum η_y around 40 mm. This information will be used to estimate the effects on on anomalous eta errors.

Table I.

Rolls and Design Vertical Off-Energy Functions of the North Arc⁽⁴⁾.

Achromat No.	Roll (Degree)	η_y (mm)
1	-10	42
2	-8.6	40
3	0	0
4	0	0
5	0	0
6	0	0
7	5.4	22
8	0	0
9	-4.26	16
10	0.44	0
11	-0.50	0
12	7.15	30
13	0.68	0
14	-7.26	30
15	-9.33	40
16	-6.30	30
17	-9.44	40
18	-6.86	30
19	-8.63	40
20	-9.66	40
21	0	0
22	10.75	42
23	9.37	40

II. The Perturbed Off-Energy Functions with Coupling

Consider that a particle of momentum p_o is launched into the arc and determines some 'central' trajectory (corresponding to a 'closed orbit' in a ring). Notice that the CT (central trajectory) is not necessarily the same as the design trajectory. Let's now consider the trajectories that are displaced from the CT and let x and y be the amount of the lateral displacement. If we keep only terms to first order in x, y , and $\Delta p/p_o$, the equations of motion for the transverse displacements of a nearby particle with respect to the CT are

$$\begin{aligned}x'' &= G_x (\Delta p/p_o) - K_x x - Qy \\y'' &= G_y (\Delta p/p_o) - K_y y - Qx\end{aligned}\tag{7}$$

The curvature function $G(s)$ is proportional to the transverse field:

$$G_x = \frac{e}{p_o} B_y \quad ; \quad G_y = -\frac{e}{p_o} B_x\tag{8}$$

The focussing strength K_x and K_y are proportional to the quadrupole strength:

$$K_x = \frac{e}{p_o} \frac{\partial B_y}{\partial x}; \quad K_y = -K_x\tag{9}$$

and the coupling term Q is proportional to the skew quadrupole strength:

$$Q = \frac{e}{p_o} \frac{\partial B_y}{\partial y}\tag{10}$$

The fields and derivatives are all to be evaluated at the CT.

The off-energy function is a particular trajectory for which $x = \eta_x(\Delta p/p_o)$ and $y = \eta_y(\Delta p/p_o)$ - - with suitable initial conditions. Using Eq. (7), we see that η will satisfy

$$\eta_x'' + K_x \eta_x = G_x - Q\eta_y$$

$$\eta_y'' + K_y \eta_y = G_y - Q\eta_x \quad (11)$$

The eta-functions are 'betatron-like' oscillations driven by (a) curvature and (b) by coupling from the eta-function in the other coordinate.

Now, suppose that in any one achromat the design trajectory is defined by $G_x = G_o, G_y = 0, K_x = K_o$ and $Q = 0$. (Local coordinates are used.) And, with respect to this trajectory, the off-energy functions are η_{ox} and η_{oy} . Now the CT of the real machine will have different fields and derivatives and a different η . Let's define the perturbed orbit functions with respect to the CT by

$$\begin{aligned} G_x &= G_o + \delta\bar{G}_x & G_y &= \delta\bar{G}_y \\ K &= K_o + \delta\bar{K} & Q &= \delta\bar{Q} \end{aligned} \quad (12)$$

They will give a perturbed off-energy function

$$\eta_x = \eta_{ox} + \bar{\eta}_x; \quad \eta_y = \eta_{oy} + \bar{\eta}_y \quad (13)$$

The overline on $\delta\bar{G}, \delta\bar{K}$ and $\delta\bar{Q}$ is to emphasize that they apply to values taken on the disturbed CT. Note that we have chosen to write the change in η as $\bar{\eta}$ (rather than as $\delta\bar{\eta}$).

If we now insert (12) and (13) into (11), we find that the anomaly $\bar{\eta}$ satisfies

$$\begin{aligned} \bar{\eta}_x'' + K_x \bar{\eta}_x &= \delta\bar{G}_x - \eta_{ox} \delta\bar{K}_x - \eta_{oy} \delta\bar{Q} = f_x \\ \bar{\eta}_y'' + K_y \bar{\eta}_y &= \delta\bar{G}_y - \eta_{oy} \delta\bar{K}_y - \eta_{ox} \delta\bar{Q} = f_y \end{aligned} \quad (14)$$

with $\delta\bar{K}_x = \delta\bar{K} = -\delta\bar{K}_y$. The perturbation $\bar{\eta}_x$ is again a betatron-like oscillation, driven now by f_x which is a sum of three parts: a perturbed field

term $\delta\bar{G}$, a perturbed gradient term $\eta_o \delta\bar{K}$ and a coupling term $\eta_o \delta\bar{Q}$, and similarly for $\bar{\eta}_y$.

If we are given a set of field perturbations we can solve Eq. (14) to get the anomaly $\bar{\eta}$.

III.Excitation of Eta by Trajectory Errors

We want to consider now the field perturbations that arise when the CT does not go through the center of a magnet. At a point whose horizontal and vertical distances from the ideal axis of an arc magnet are X and Y , the magnetic field of the Arc magnet is given by

$$B_y = B_o + \kappa_o X + \frac{1}{2} S(X^2 - Y^2)$$

$$B_x = \kappa_o Y + S X Y \quad (15)$$

with

$$\kappa_o = \frac{dB_y}{dX}, \quad S = \frac{d^2 B_y}{dX^2} \quad (16)$$

are the quadrupole and sextupole components. At the design energy of 50 GeV, the field values are $B_o = 5.97KG$, $\kappa_o = \pm 7.02KG/cm$ and $S = 1.63KG/cm^2$ for focus and $-2.70KG/cm^2$ for defocus magnets. If the CT passes through such a magnet at the displacement $\bar{\delta x}, \bar{\delta y}$ from the axis, the disturbed field functions, to first order in $\bar{\delta x}$ and $\bar{\delta y}$, are

$$\bar{B}_y = B_o + \kappa_o \bar{\delta x}$$

$$\bar{B}_x = \kappa_o \bar{\delta y}$$

$$\left(\frac{\partial B_y}{\partial X}\right)_{CT} = \kappa_o + S \bar{\delta x}$$

$$\left(\frac{\partial B_y}{\partial Y}\right)_{CT} = S \bar{\delta y} \quad (17)$$

making use of Eqs. (8) and (9), we find that

$$\delta \bar{G}_x = K_o \bar{\delta x}$$

$$\delta G_y = -K_o \bar{\delta y}$$

$$\delta K_x = \mu \bar{\delta x} = -\delta K_y$$

$$\delta \bar{Q} = -\mu \bar{\delta y} \quad (18)$$

where $\mu = (e/p_o) S$ is the normalized sextupole strength. Here we want to remind the reader that the coordinate of a particle from magnet centerline X is made up by the distance of the particle to CT, x , and the distance from CT to magnet centerline $\bar{\delta x}$. In other words, $X = \bar{\delta x} + x$ and $Y = \bar{\delta y} + y$

The driving functions f_x and f_y of Eq. (14) due to orbit errors $\bar{\delta x}$ and $\bar{\delta y}$ are

$$f_x = (K_o - \eta_{ox} \mu) \bar{\delta x} + \eta_{oy} \mu \bar{\delta y}$$

$$f_y = -(K_o - \eta_{ox} \mu) \bar{\delta y} + \eta_{oy} \mu \bar{\delta x} \quad (19)$$

The expression for f_x differs from the corresponding expression of CN-333⁽²⁾ by the new coupling term $\eta_{oy} \mu \bar{\delta y}$. (In that report, we considered only plane geometries, so η_{oy} was taken to be zero.)

We call your attention to the strange asymmetry between the expressions for f_x and f_y . The second term in f_y arises from the coupling from η_{ox} to η_y . And, the third term in f_y comes from the gradient change - - which is in the second term of f_x !

Now the sextupole strengths μ of the arc magnet have been chosen to make an achromatic system for which, it turns out, the expression $(K_o - \eta_{ox} \mu)$ that appears in Eq. (19) is, when averaged over a magnet very closely equal to zero. [See the discussions in CN-333⁽²⁾ and CN-343⁽⁵⁾.] So, for the arc magnets, the resulting driving terms for $\bar{\eta}$ reduce to

$$f_x = (\eta_{oy} \mu) \bar{\delta y}$$

$$f_y = (\eta_{ox} \mu) \bar{\delta x} \quad (20)$$

Our important conclusion is that alignment errors will drive errors in both η_x and η_y in any region of the arcs in which the design vertical eta, η_{oy} is not zero. Since the design of the arcs calls for rolled achromats in which there is a rather large η_{oy} , we must expect to find an anomalous eta driven by alignment errors. We note that a similar conclusion has been reached by T. Fieguth, S. Kheifets and J. Murray using computer tracking, see CN-343⁽⁵⁾.

In the next Section we estimate the magnitude of the anomalous eta expected from random alignment errors.

IV. Anomalous Eta after Steering Corrections

We now estimate the magnitude of the anomalous eta expected from random alignment errors in the arcs. We will carry out the analysis in detail for $\bar{\eta}_x$. The extension to $\bar{\eta}_y$ is straightforward. From Eqs. (14) and (20) the anomalous eta satisfies

$$\bar{\eta}''_x + K_x \bar{\eta}_x = \eta_{oy} \mu \bar{\delta y} \quad (21)$$

when $\bar{\delta y}$ stands for the displacement of the disturbed central trajectory (CT) from the magnet axis. We now make the following approximations. We treat the effect of each magnet as an impulsive perturbation placed at its center, and

take that the magnet produces, using Eq. (21), a slope change in $\bar{\eta}_x$ of

$$\Delta\bar{\eta}'_{xi} = \eta_{oyi} \mu_i \overline{\delta y_i} \ell \quad (22)$$

where $\overline{\delta y_i}$ is the (mean) trajectory displacement in the i -th magnet, μ_i is its sextupole strength, η_{oyi} is the typical value of the undisturbed vertical eta in the magnet, and ℓ is the magnet length.

Such an impulsive perturbation produces downstream a free oscillation of $\bar{\eta}_x$ described by

$$\bar{\eta}_{xi} = a_{xi} \sqrt{\beta_x} \sin(\phi_x - \phi_i) \quad (23)$$

where β_x and ϕ are taken at the observation point. The invariant amplitude a_i produced by (22) is

$$a_{xi} = \sqrt{\beta_{xi}} \Delta\bar{\eta}'_{xi} = \sqrt{\beta_{xi}} \eta_{oyi} \mu_i \overline{\delta y_i} \ell \quad (24)$$

The a_{xi} are, of course, random variables, so we can only inquire about stochastic quantities. We ask in particular for a representative value for the total amplitude a at the end of the arc - - which we take as the root-mean-square of the expected a .

The statistical analysis in this case is rather complex, because the size of the a_{xi} is correlated with their phases ϕ_i . It is, however, possible to show that so long as the δy_i are not correlated with magnet position, the total amplitude is still the usual random walk with a resulting root-mean-square given by

$$(a_x)_{rms} = \sqrt{N} \ell \langle \beta_{xi} \eta_{oyi}^2 \mu_i^2 \rangle^{\frac{1}{2}} \overline{\delta y_{rms}} \quad (25)$$

The quantity in the brackets is quite deterministic - - being given by the arc design. It only remains to determine its average value throughout the arc.

It is probably more useful to give some typical value of $\bar{\eta}_x$ at the end of the arc rather than a_x . We chose to take as our measure the rms value of the peak value of $\bar{\eta}_x$ in the last achromat - - written as $(\hat{\eta}_x)_{rms}$. In terms of $(a_x)_{rms}$

$$(\hat{\eta}_x)_{rms} = \sqrt{\hat{\beta}_x} (a_x)_{rms} \quad (26)$$

Since the arc cells are symmetric $\hat{\beta}_x = \hat{\beta}_y$ and we can drop the subscript. Then Eq. (25) becomes

$$(\hat{\eta}_x)_{rms} = \sqrt{N\hat{\beta}} \ell \langle \beta_x \eta_{oy}^2 \mu^2 \rangle^{\frac{1}{2}} \bar{\delta y}_{rms} \quad (27)$$

The nature of the bracket becomes more evident if we transform it somewhat. We defer the details to Appendix A, where it is shown that

$$\langle \beta_x \eta_{oy}^2 \mu^2 \rangle^{\frac{1}{2}} = \frac{\zeta_x (\hat{\eta}_{oy})_{rms}}{(2\hat{\beta})^{\frac{1}{2}}} \quad (28)$$

where ζ_x is a property of a cell, namely the rms value of $\sqrt{\beta_x \beta_y \mu}$:

$$\zeta_x = \langle \beta_x \beta_y \mu^2 \rangle_{cell}^{\frac{1}{2}}; \quad (29)$$

and $\hat{\eta}_{oy}$ is the peak value of η_{oy} in each achromat. (The rms value of $\hat{\eta}_{oy}$ is then an average over all achromats.) Eq. (27) then becomes

$$(\hat{\eta}_x)_{rms} = \sqrt{\frac{N}{2}} \ell \zeta_x (\hat{\eta}_{oy})_{rms} \bar{\delta y}_{rms} \quad (30)$$

This is the final form of our result.

Following through the same analysis for the anomalous vertical eta $\bar{\eta}_y$, the only changes are that β_x becomes β_y , and $\bar{\delta y}$ becomes $\bar{\delta x}$, so we get that

$$(\hat{\eta}_y)_{rms} = \sqrt{\frac{N}{2}} \ell \zeta_y (\hat{\eta}_{oy})_{rms} \bar{\delta x}_{rms} \quad (31)$$

with

$$\zeta_y = \langle \beta_y^2 \mu^2 \rangle_{cell}^{\frac{1}{2}} \quad (32)$$

Notice that ζ_y has a significantly different form from ζ_x , see Eq. (29).

V. Numerical Estimates

We will make here only some rough estimates of the parameters. We obtain ζ_x and ζ_y from the following table.

Magnet	β_x (m)	β_y (m)	μ (m ⁻³)	$\beta_x \beta_y \mu^2$ (m ⁻⁴)	$\beta_y^2 \mu^2$ (m ⁻⁴)
F	7.5	1.8	9.8	1300	311
D	1.8	7.5	-16.3	3590	14950
<i>rms</i>				49 m ⁻²	87 m ⁻²

So,

$$\zeta_x \approx 49m^{-2} \text{ and } \zeta_y \approx 87m^{-2} \quad (33)$$

From the SLC Blue Book⁽⁴⁾ we can read from the graphs a rough value for the peak η_{oy} in each achromat. Taking the *rms* of these values we find that

$$(\hat{\eta}_{oy})_{rms} \approx 28 \text{ mm} \quad (34)$$

(More accurate calculations of these numbers could of course be made!)

For the arcs $N = 450$ and $\ell = 2.5m$. If we assume the standard alignment tolerance of $10^{-4}m$ the *rms* displacements $\bar{\delta}x$ and $\bar{\delta}y$ are $1.5 \times 10^{-4}m$. (See A. Chao and W. Weng: CN-254.⁽⁶⁾). We then get the following estimates for the expected anomalous eta:

$$(\hat{\eta}_x)_{rms} \approx 8 \text{ mm}, \quad (\hat{\eta}_y)_{rms} = 14 \text{ mm} \quad (35)$$

If expressed in terms of the percentage deviation from the designed maximum etas, they are

$$(\hat{\eta}_x)_{rms}/\hat{\eta}_{ox} = 19\% \quad \text{and} \quad (\hat{\eta}_y)_{rms}/\hat{\eta}_{oy} = 33\% \quad (36)$$

VI. Discussion

We wish to make several observations about our results.

1. Because of the rolled achromats in the arcs, we expect a perturbation to the dispersion function η , due to residual alignment errors, which is not small - - particularly for η_y . Typical values of the design eta are of the order of 20 to 45 mm, and, of course, η_y is designed to be zero through much of the arcs and especially at the end. Our estimated $\bar{\eta}_y$ of 14 mm will constitute a major perturbation to η_y on leaving the arcs. These results agree reasonably with results of simulations that have been reported by the BDTF.⁽⁸⁾
2. Our calculation is a perturbation treatment which is valid only if the size of the anomaly $\bar{\eta}$ is sensibly less than the undisturbed η . Actually, we require mainly that η_y is somewhat less than $(\hat{\eta}_{oy})_{rms} = 28 \text{ mm}$ - - see Eq. (34). The calculated anomaly barely satisfies this requirement. It would not do so if the anomaly $\bar{\eta}_y$ were, by a fluctuation, to be twice the *rms* value. It is also evident that the approximation deteriorates if the tolerances are worse than assumed. We point out also, that when the anomalous eta gets too large the second-order contributions always act to make the anomaly still worse. The anomalous part will increase the driving term η_y , and there is a positive feedback. This observation is consistent with recent simulation results reported by K. Brown and R. Servranckx.⁽⁷⁾ Fig. 3 shows the perturbation on η_x and η_y under 100 μm random misalignments, and Fig. 4 shows the results with 300 μm misalignments. The perturbed off-energy functions shown in Figs. 3 and 4 are taken from the end of each achromat, errors

inside the magnets should be larger. The results shown in Figs.3 and 4 are from one particular seed of misalignment. For different seeds the pattern can vary, but the general features, interpreted statistically, remain.

3. The calculated $\bar{\eta}_y$ is larger than $\bar{\eta}_x$ by the factor $\zeta_x/\zeta_y = 1.8$ (This effect comes about because the driving term is proportional to η_{oy} and hence to $\sqrt{\beta_y}$ while the sensitivity of $\bar{\eta}$ to the perturbation is proportional to $\sqrt{\beta_x}$ for $\bar{\eta}_x$ and to $\sqrt{\beta_y}$ for $\bar{\eta}_y$. Now β_x and β_y oscillate out of phase so β_y^2 is always larger than $\beta_x\beta_y$, and so, also, is its average.) This result is also in accord with recent simulation studies.
4. The anomalous vertical eta, through synchrotron radiation, may contribute a significant increase in the vertical emittance which cannot be restored by the optical correction system provided for at the Final Focus. A preliminary estimate indicates that the expected vertical emittance might nearly be doubled. This effect should be studied further.
5. Our analyses assume that the residual misalignment $\bar{\delta x}$ and $\bar{\delta y}$ are pure random numbers. We know that the beam steering procedure in the arcs certainly modifies the distribution of magnet position errors so that they are forced to be correlated in such a way that the central trajectory is constrained to have small displacements. We have looked at this matter briefly and believe that the residual misalignments $\bar{\delta x}, \bar{\delta y}$ which remain after steering are effectively random for their effect on the anomalous eta.
6. The fact that magnet displacements can generate an anomalous eta opens the possibility that the magnet movers might be exploited for the correction of η within the arcs. Such a correction system should be able to affect beta function and eta-function orthogonally without damaging the orbit.
7. Another possible source for generating η_{oy} is the error of phase advance in one achromat created by systematic gradient error in the arc. Such an error will make the transfer matrix within one achromat differ from unity

and consequently makes the cancellation of roll at the end of the achromat incomplete. The resultant eta error and the effect on anomalous eta perturbation should be studied further.

Acknowledgements

The authors would like to thank K. Brown, T. Fieguth, H. Hutton, P. Morton and R. Servranckx for helpful discussions.

REFERENCES

1. M. Sands, "The Physics of Electron Storage Rings, An Introduction," SLAC-121, November 1970.
2. M. Sands and W. Weng, "Perturbations to the Horizontal Off-Energy Functions in the Arcs," SLAC CN-333, July 1986.
3. K. Brown, F. Rothacker, D. Carey, C. Iselin, TRANSPORT, SLAC-91, Rev. 2., May 1977.
4. SLC Design Handbook, SLAC, December 1984.
5. T. Fieguth, S. Kheifets and J. J. Murray, "Dispersive Effects of Transverse Magnet Displacements in Rolled Arc Achromats," SLAC-CN-343, September 22, 1986.
6. A. Chao and W. Weng, "An Attempt to Compare Two Arc Orbit Correction Scheme Analytically," SLAC-CN-254, December 1983.
7. R. Servranckx and K. Brown, private communications and CN note to be published.
8. S. Kheifets, T. Fieguth, K. L. Brown, A. Chao, J. J. Murray, R. V. Servranckx and H. Widemann, "Beam Optical Design and Studies of the SLC Arcs," SLAC-PUB-4013, June 1986 and T. Fieguth, "GIAT-NOTE," Aug. 7, 1984.

APPENDIX A

We wish to transform the quantity $\beta_x \eta_{oy}^2 \mu^2$ to a more convenient form in order to facilitate finding its average. Notice that β_x and μ oscillate with a cell period while η_{oy} oscillates with a period of $3\frac{1}{3}$ cells in each achromat and has a different amplitude in each achromat. To find the average, it is convenient, first to find the average over any one achromat, and then to average over the achromats.

In any one achromat, say the k -th achromat, we can write that

$$\eta_{oy} = \frac{(\hat{\eta}_{oy})_k}{\sqrt{\hat{\beta}_y}} \sqrt{\beta_y} \cos(\phi - \theta_k) \quad (A.1)$$

where $(\hat{\eta}_{oy})_k$ is the peak value of η_{oy} and θ_k is the phase of its oscillation. Both constants are determined by the achromat roll pattern up to the k -th achromat. $\hat{\beta}_y = \hat{\beta}_x = \hat{\beta}$ is the same in all achromats.

Since there are 3 betatron oscillations in one achromat and ten cells, it is easy to show that the correlation between the cosine factor and the value of β_x, β_y and μ averages to zero, so that we can take the mean square of $\cos(\phi_i - \theta_i)$ equal to one-half. Since $(\hat{\eta}_{oy})_k$ and $\hat{\beta}$ are constant in the k -th achromat, the average for that achromat becomes

$$\langle \beta_x \eta_{oy}^2 \mu^2 \rangle_k = \frac{\langle \beta_x \beta_y \mu^2 \rangle (\hat{\eta}_{oy})^2 k}{2\hat{\beta}} \quad (A.2)$$

The quantity $\beta_x \beta_y \mu^2$ has a period of one cell, and so its average is just the cell average - - a number that is characteristic of the cell and which we write as ζ_x^2 ,

$$\zeta_x^2 = \langle \beta_x \beta_y \mu^2 \rangle \quad (A.3)$$

The arc rms for the bracket is then just $\zeta/\sqrt{2\hat{\beta}}$ times the *rms* value of the

individual achromat amplitudes $(\hat{\eta}_{oy})_k$. Define

$$(\eta_{oy})_{rms} = [\sum_k (\eta_{oy})_k^2]^{\frac{1}{2}} \quad (A.4)$$

Putting it together we get Eq. (27) in the body of the report.

ARCN FINAL (12-27-83): BEGINNING TO 1000 FEET

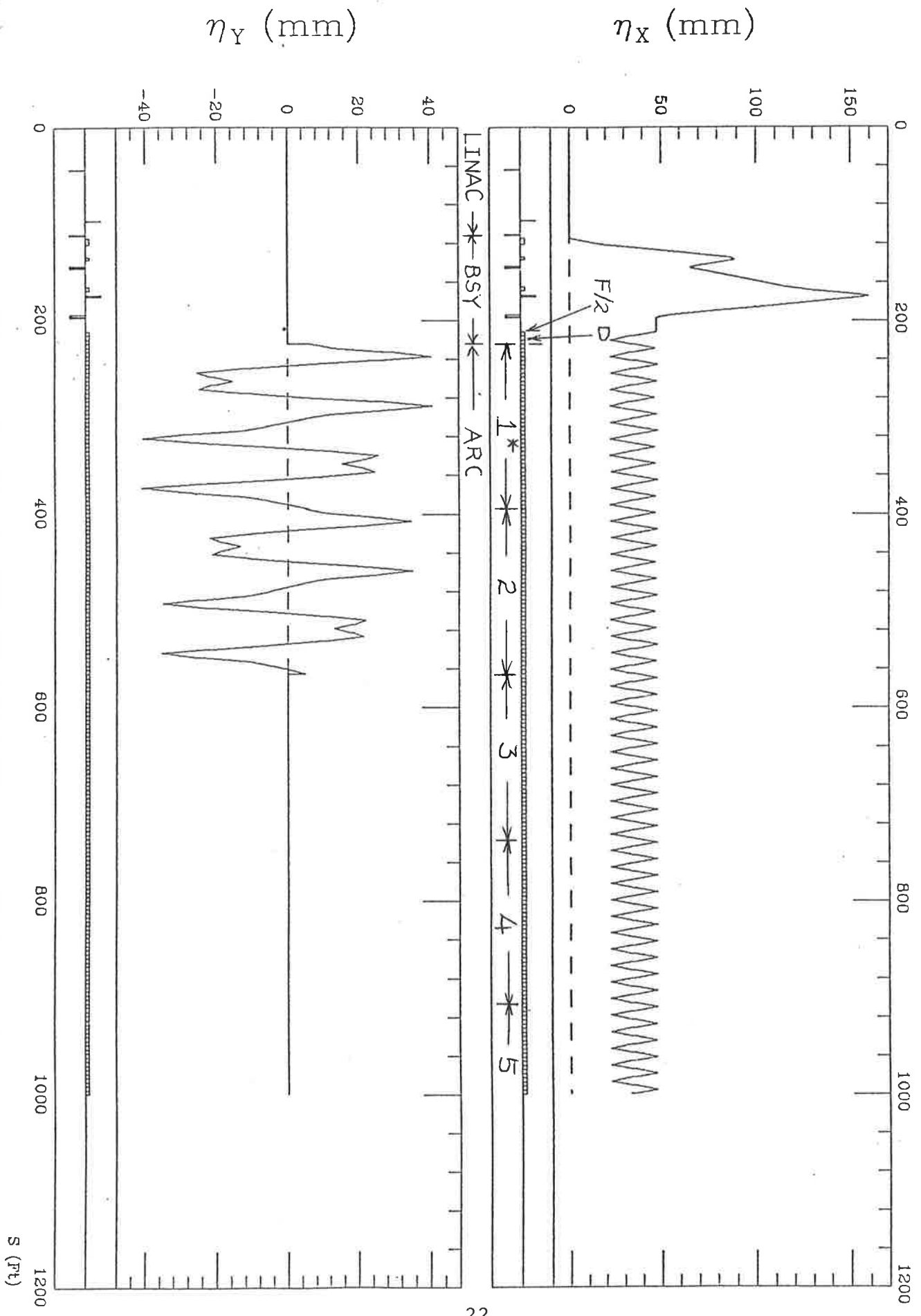


Fig.1a The unperturbed off-energy functions of the north Arc
 (* achromat numbers used in table I)

ARCN FINAL (12-27-83): 1000 FEET TO 2000 FEET

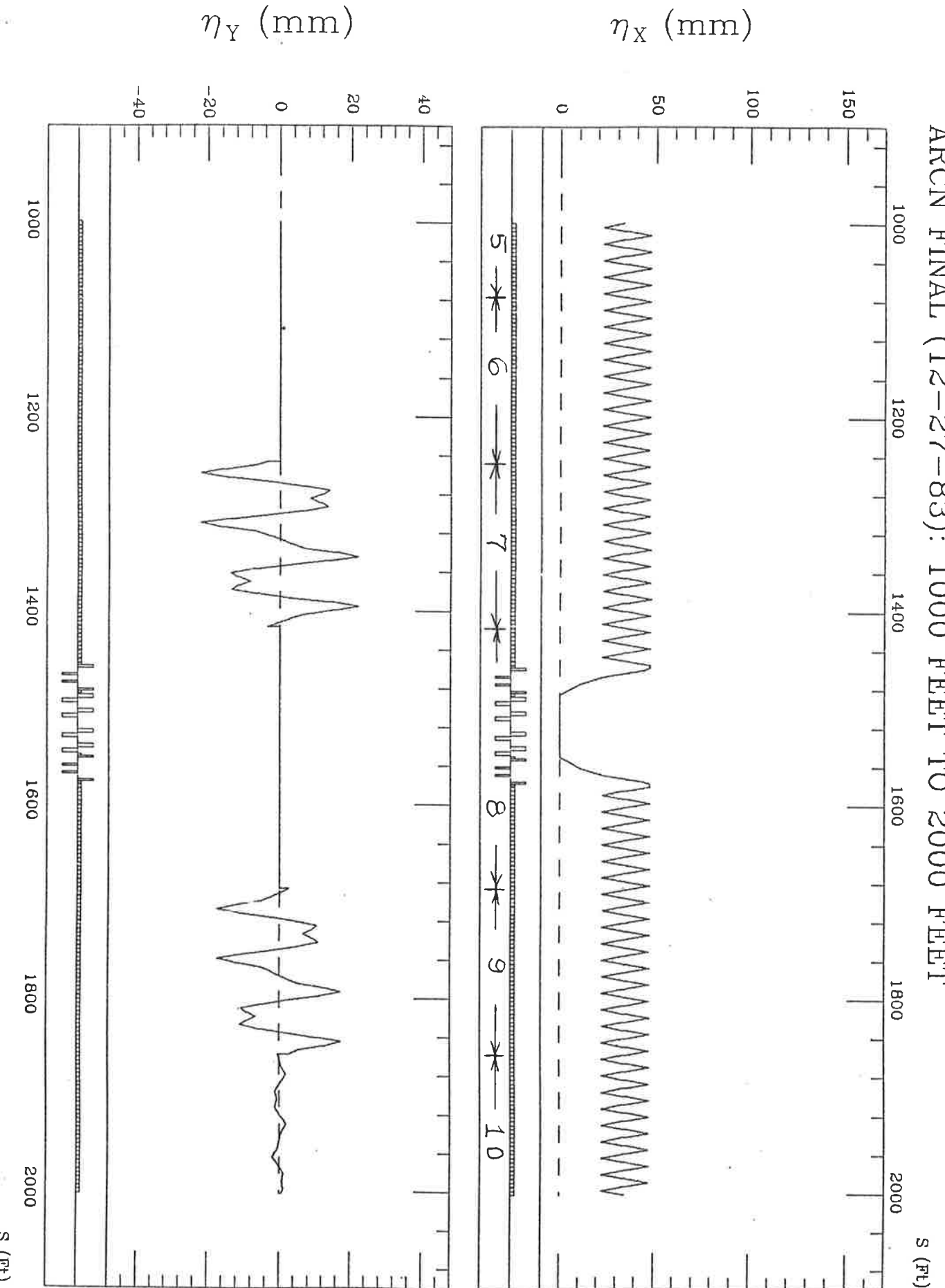


Fig. 1b

S (Ft)

ARCN FINAL (12-27-83): 2000 FEET TO 3000 FEET

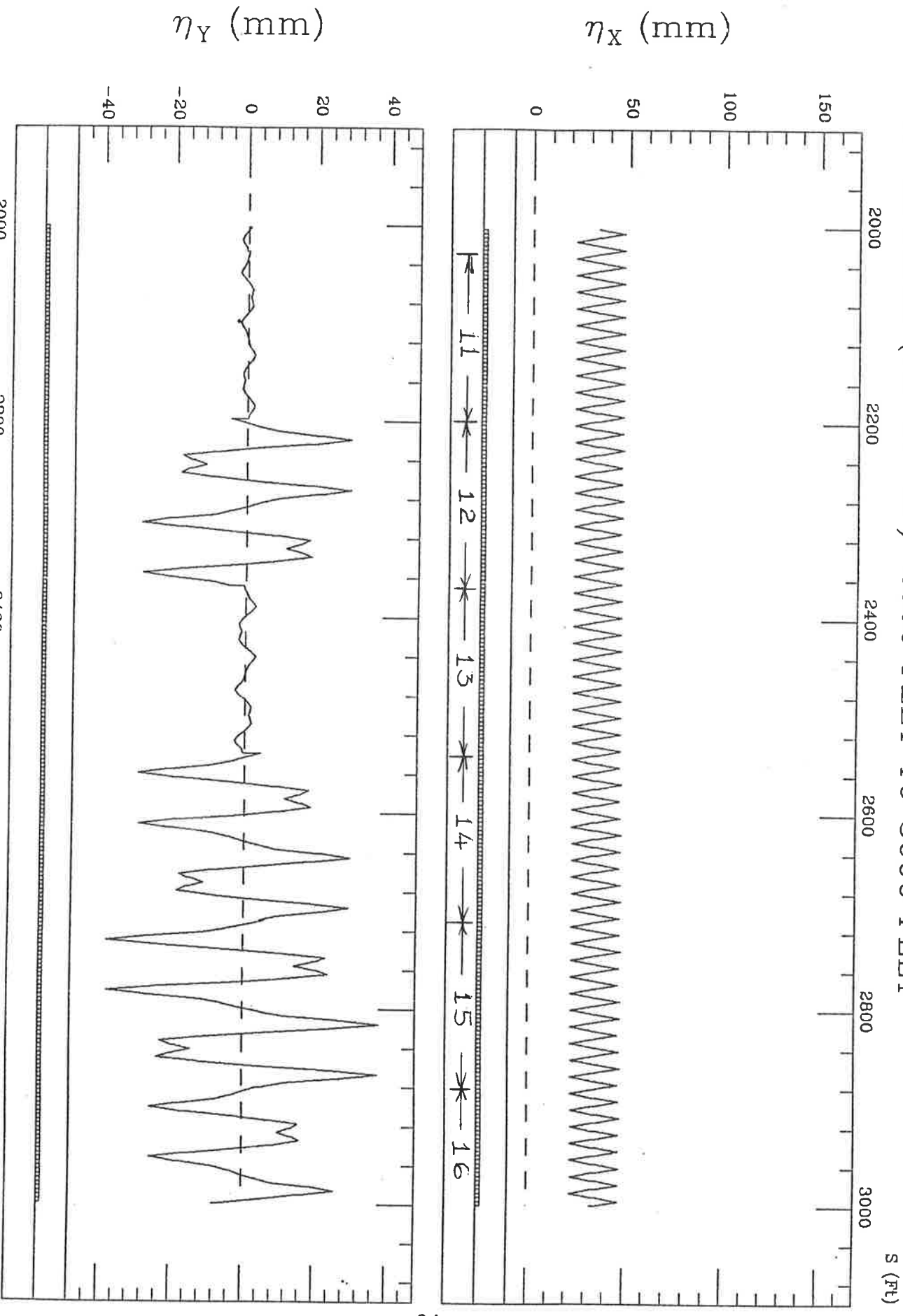
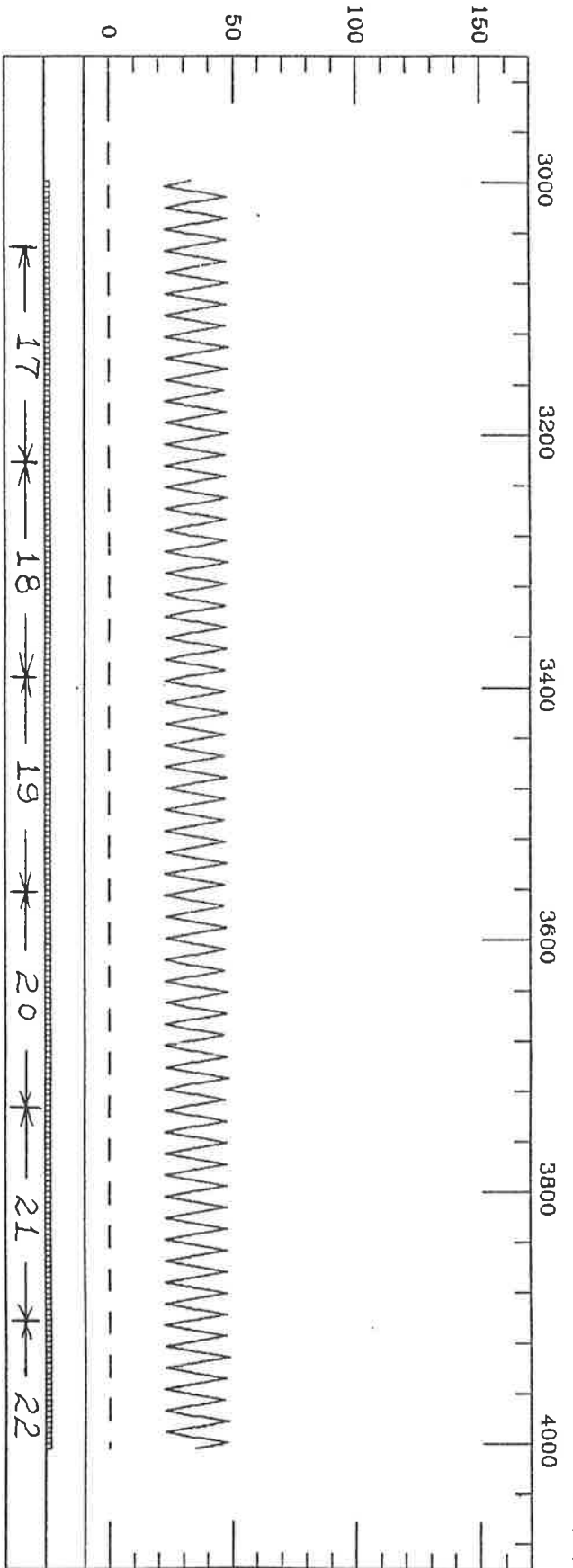


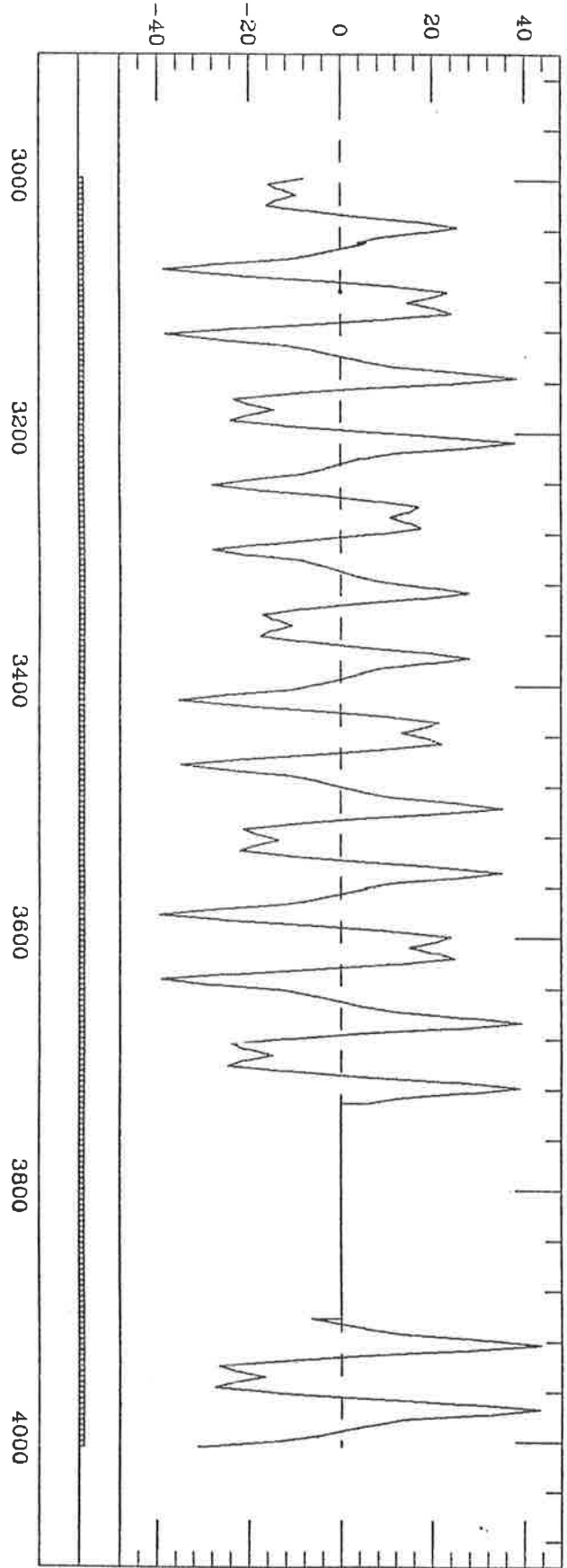
Fig. 1c

ARCN FINAL (12-27-83): 3000 FEET TO 4000 FEET

S (Ft)



η_Y (mm)



S (Ft)

Fig. 1d

ARCN FINAL (12-27-83): 4000 FEET TO ARC END

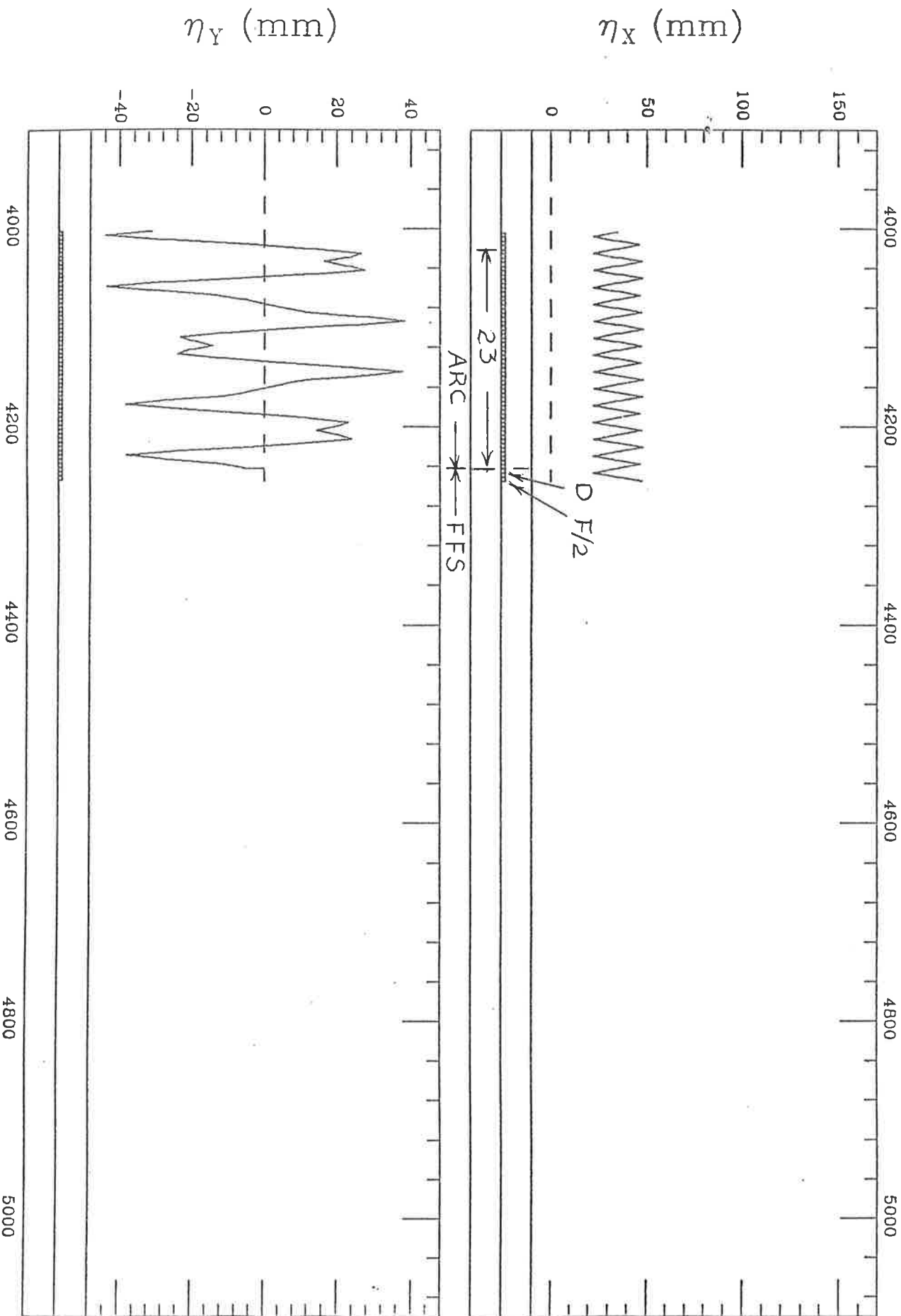


Fig. 1e

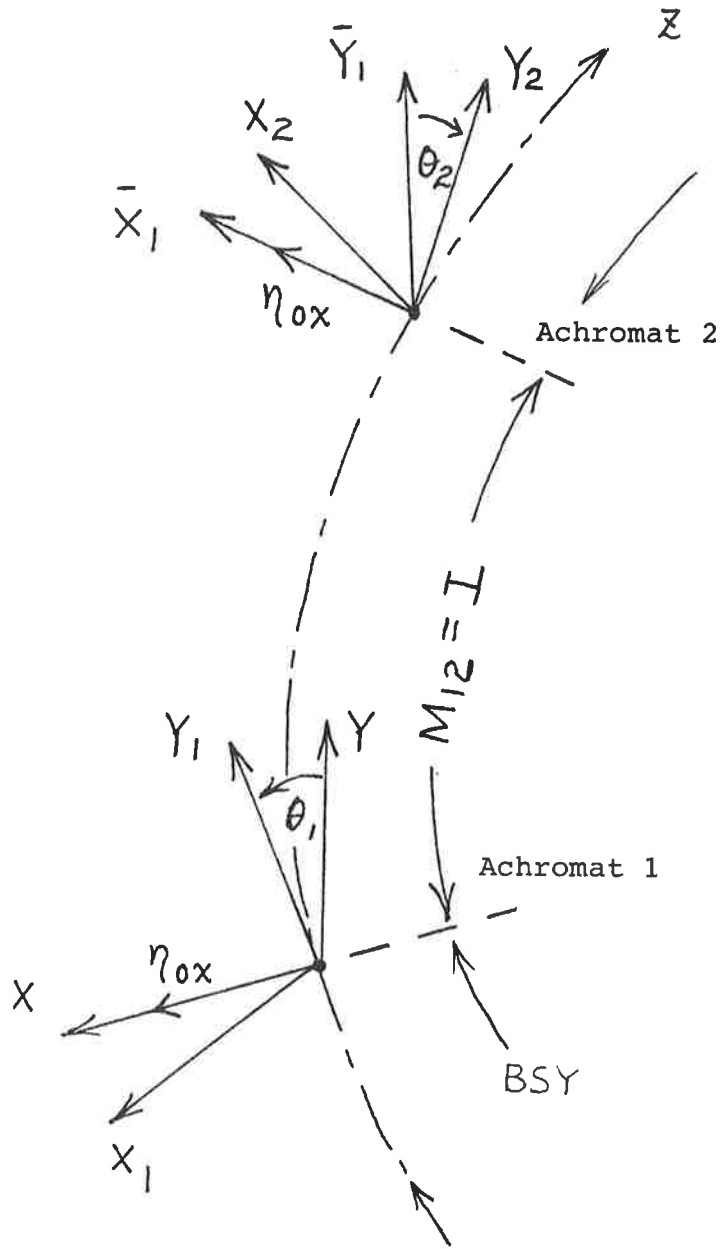


Fig. 2 The rolls and coordinate systems of achromat 1 and 2

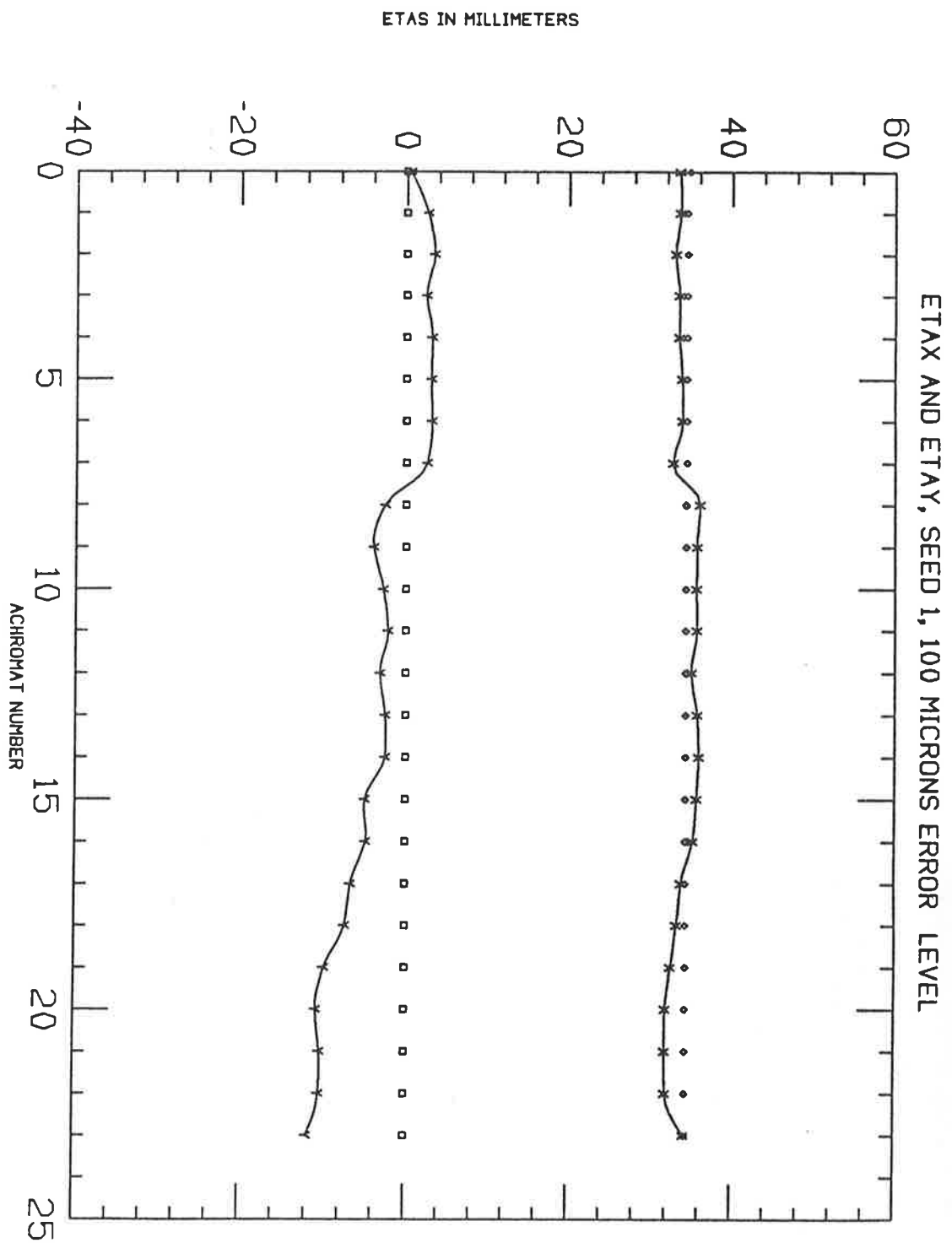


Fig. 3 The perturbed off-energy functions with 100 microns misalignment. (Ref. 7)

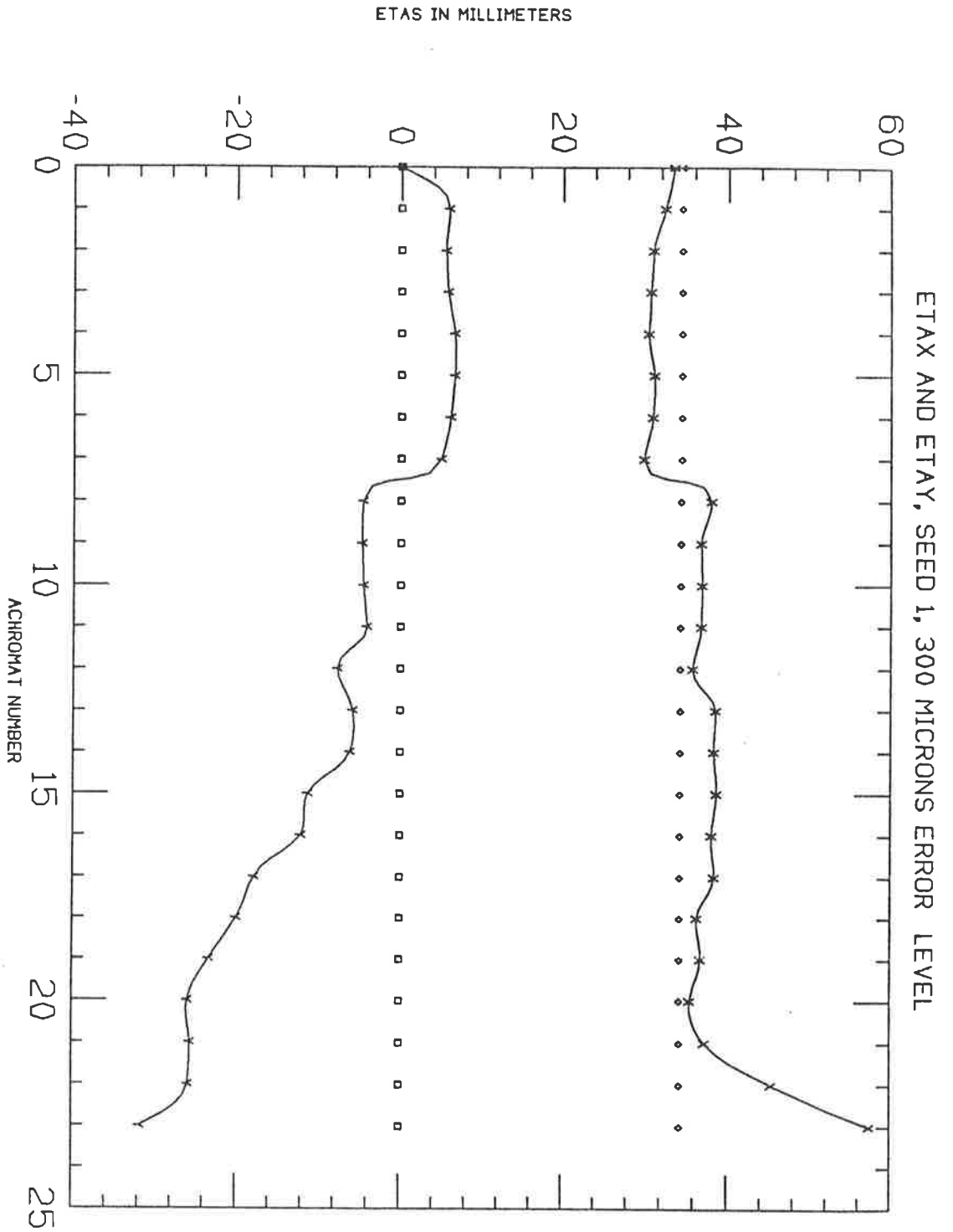


Fig. 4 The perturbed off-energy functions
with 300 microns misalignment. (Ref. 7)